We are IntechOpen,
the world's leading publisher of
Open Access books
Built by scientists, for scientists

6,900
Open access books available

186,000
International authors and editors

200M
Downloads

154
Countries delivered to

Our authors are among the

TOP 1%
most cited scientists

12.2%
Contributors from top 500 universities

CLARIVATE ANALYTICS
BOOK CITATION INDEX
INDEXED

WEB OF SCIENCE™

Selection of our books indexed in the Book Citation Index
in Web of Science™ Core Collection (BKCI)

Interested in publishing with us?
Contact book.department@intechopen.com

ECG Ambulatory System for Long Term Monitoring of Heart Rate Dynamics

Agustín Márquez-Espinoza, José G. Mercado-Rojas,
Gabriel Vega-Martínez and Carlos Alvarado-Serrano
CINVESTAV,
México

1. Introduction

Poor eating habits, a sedentary life style, and smoking have made acute coronary syndrome a disease characteristic of modern life, that it is expected to be the primary cause of death in the world by the year 2020, in spite of the development of reperfusion therapy and the use of defibrillators (Fuster, 2002). At the present time, cardiovascular diseases (CVDs) are the number one cause of death globally, and according to World Health Organization (WHO), an estimated 17.1 million people died of CVDs in 2004, representing 29% percent of all global deaths. Of these deaths, an estimated 7.2 million were due to coronary heart disease (CHD) (WHO, 2011). In Mexico, CVDs are the main cause of death, and the most frequent form is the ischemic heart disease (Instituto Nacional de Estadística, Geografía e Informática [INEGI], 2010).

CHD involves a reduction in the blood supply to the myocardium by narrowing or blocking of the coronary arteries, so the cells in the region served by the vessel will behave abnormally due to hypoxia (myocardial ischemia) or may die (myocardial infarction). These abnormalities due to neuronal damage and metabolic derangements cause alterations in sympathetic and parasympathetic flow to the heart, leading to increased heterogeneity of ventricular repolarization and to the development of terminal arrhythmias (Metha, 1997).

Therefore, the use and development of noninvasive techniques as electrocardiography, that records the electrical activity generated by the muscles of the heart in the surface on the body, opens a useful perspective for diagnosis and treatment in patients with heart diseases as the ischemia and infarction. The electrocardiogram (ECG) is the waveform produced by this electrical activity of the heart and its generation depends of four electrophysiological processes: the formation of electrical impulse in the main heart pacemaker (sinoatrial node), the transmission of this impulse through specialized fibers in the conduction, the activation (depolarization) and the recovery (repolarization) of the myocardium.

The electrical activity generated by the heart can be modeled as a vector whose magnitude and direction changes throughout the cardiac cycle. To record the different projections of

this vector, several electrodes are attached to the body in different locations known as leads.

Because each lead measures the ECG between two points from different directions, amplitudes, polarities, times and durations of the ECG components vary between leads, so these have been standardized. The lead system most accepted in clinical practice is the standard 12 lead system, that is the combination of the bipolar limb leads I, II and III, the augmented unipolar limb leads aVR, aVL and aVF, and the six unipolar precordial leads V1-V6. Limb leads (I, II, III) derive signals from the left arm (LA), the right arm (RA) and the left leg (LL). The right leg (RL) electrode is the common reference in the amplifier.

The augmented signals (aVR, aVL, aVF) were proposed by Goldberger and derive signals from the limb leads. The unipolar chest leads were proposed by Wilson, and derive signals from six different chest locations, in where the common reference is the Wilson central terminal, that is formed by a resistive network that contributes equally weighted signals from each of the LA, RA and LL electrodes (Thakor 1988). Waves, segments and intervals of the ECG are shown in the Fig. 1.
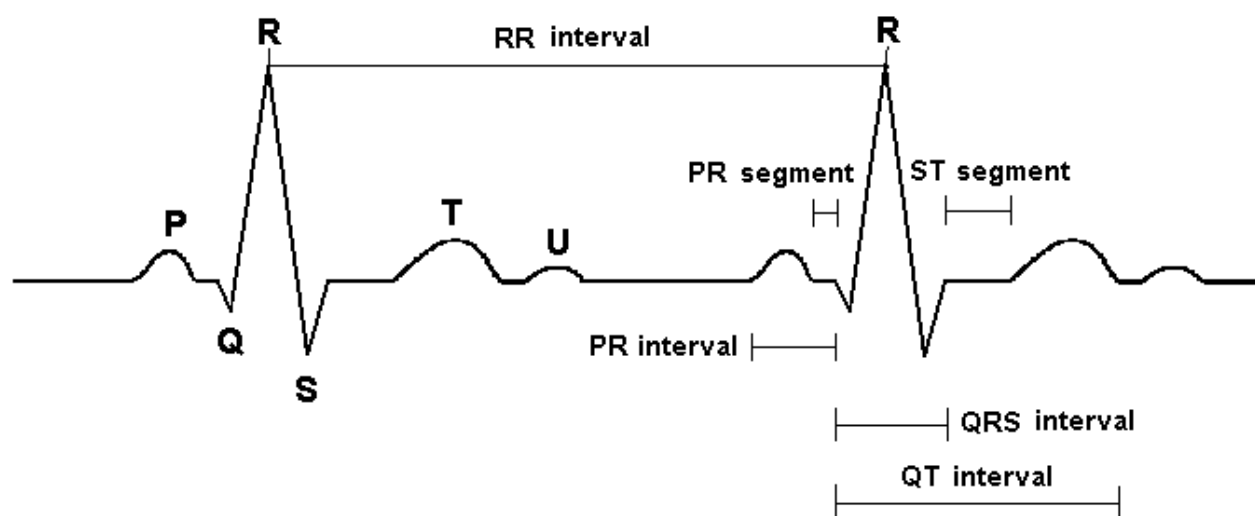

Fig. 1. Waves, intervals and segments of the ECG

The P, QRS, and T waves reflect the rhythmic electrical depolarization and repolarization of the myocardium associated with the contractions of the atria and ventricles. The P wave represents depolarization of the atrial musculature. The QRS complex is the combined result of the repolarization of the atria and the depolarization of the ventricules, which occur almost simultaneously. The T wave represents repolarization of the ventricles, whereas the U wave, if present, is believed to be the result of after-potentials in the ventricular muscle. Time intervals defined by the onsets and ends of these waves are important in electrocardiographic diagnosis because reflect electrophysiological processes of heart and autonomic nervous system (ANS), and carry clinical implications when they lie outside the range of the normal variation.

The most important intervals are the PQ interval, the QRS interval, the ST segment, the QT interval and the RR interval. The PQ interval reflects in part the atrioventricular conduction time. The QRS interval is a measure of the total duration of depolarization of ventricular

tissue. The ST segment represents the end of ventricular depolarization and the onset of ventricular repolarization. The QT interval reflects the total period of ventricular depolarization and repolarization. The RR interval is the interval between consecutive heart beats and determines heart rate.

The intervals that detect the following pathological conditions: slowed conduction (QRS interval), heterogeneities in ventricular repolarization (QT interval and QT dispersion [maximal difference of QT intervals between leads]), and imbalance in autonomic tone (temporal variation in the RR intervals named heart rate variability [HRV]), are considered as noninvasive risk stratification parameters for identifying patients with coronary artery disease who are at risk for sudden cardiac death (Goldberger et al., 2008).

Because a standard ECG provides only a fixed picture of 12 leads portraying cardiac electrical events over a brief duration, there is a need for continuous ECG recording over long periods of time, due to certain abnormalities may occur only during sleep or with mental, emotional, or exercise-induced changes in cardiac oxygenation or function. The technique of continuous ECG recording or long term ECG (typically used for 24 to 48 h) with ambulatory ECG monitors (also termed Holter monitors), is used in clinical practice to detect, document, and characterize occurrences of abnormal cardiac electrical behavior of the heart during ordinary daily activities (Kadish et al., 2001).

The major uses of long term ECG are in the diagnosis and assessment of cardiac symptoms, the prognostic assessment or risk stratification of cardiac disease populations and the evaluation of therapeutic interventions. The use of Holter recordings for risk stratification of cardiac populations has used parameters like ST segment changes (for myocardial ischemia), RR interval changes (for HRV) and QT interval measurements [for repolarization abnormalities] (Kennedy, 2004).

This chapter describes the development of a prototype of a telemetry ambulatory system of long-term of 3-lead ECG and algorithms for detection of R wave peak of ECG and processing of RR intervals implemented in LabVIEW® for the study of heart rate dynamics.

2. Methodology

The basic requirements considered for the ECG telemetry ambulatory system design are:
- RF Wireless communication
- Low power consumption
- Small size
- Battery operated for a minimum continuous operation of 24 h
- Low battery voltage detection
- Simultaneous acquisition of three ECG leads: DI, aVF and V2, and battery information
- Recording, display and storage in real time of three ECG leads and battery information in a PC with an interface developed in Lab VIEW

The proposed system is composed of two blocks: a transmitter and a receiver (Fig. 2). Tasks of the transmitter are conditioning, digitalization, processing, encoding and simultaneous RF transmission of 3 ECG leads and battery information to the receiver. In the receiver, the transmitted ECG signals are detected, decoded, and sent to USB port or serial port in the PC for recording, storage and display.
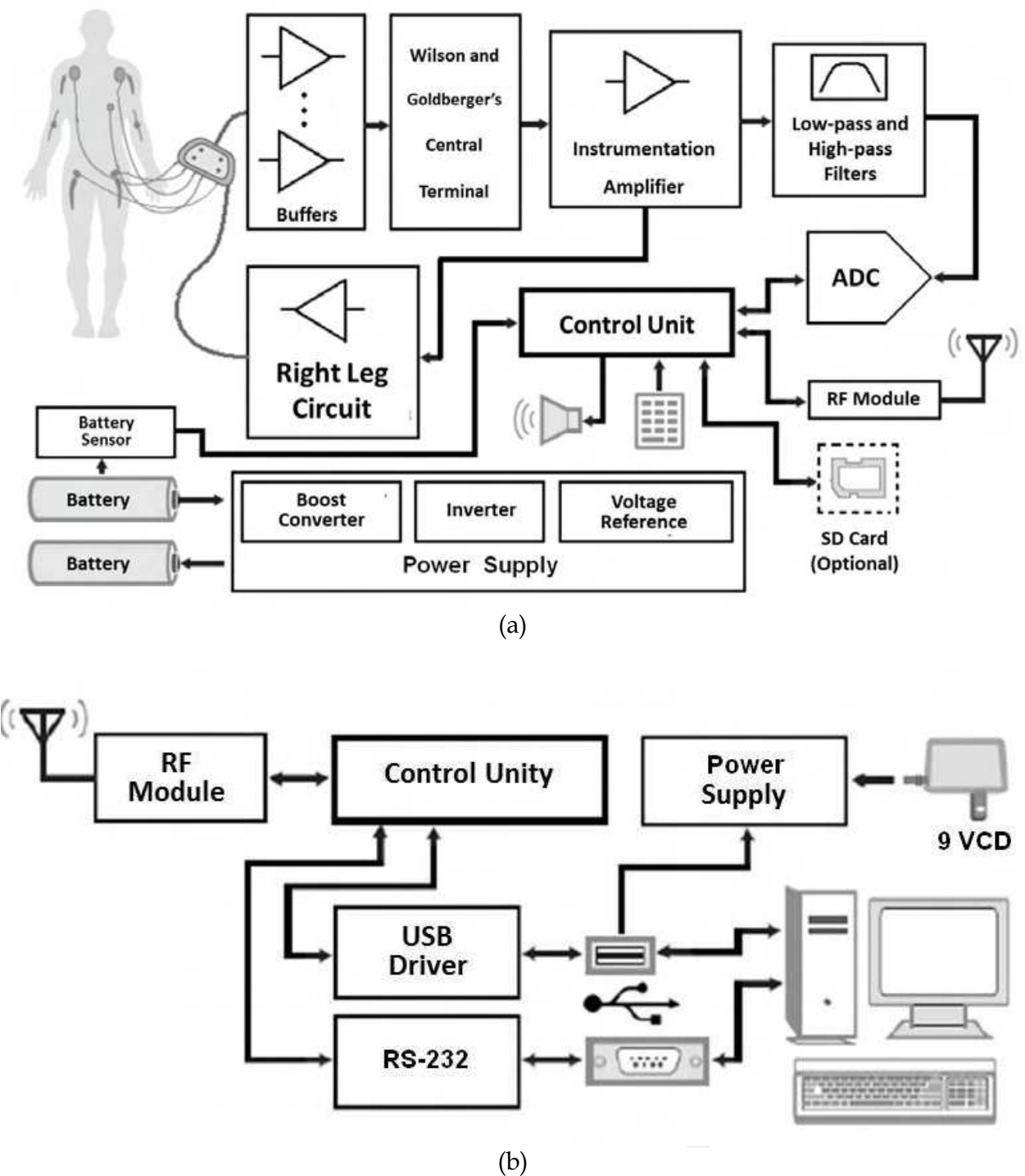
(a)

(b)

Fig. 2. ECG telemetry ambulatory system block diagram (a) Transmitter. (b) Receiver.

2.1 Transmitter
2.1.1 Conditioning stage

The main function in this stage is to amplify ECG signal in selected leads without distortion, and to minimize noise and interference, because an inadequate low-frequency response of ECG amplifier introduces artificial distortion in the level of ST segment (Christov et al. 1997).

This stage consists of the buffers section, the resistors network of central terminals of Wilson and Goldberger and three ECG amplifiers for three leads. Lead system used is of 5 electrodes, where 4 electrodes are placed in the LA, RA, LL and RL positions, and 1 electrode can be placed in any of the standard V1 to V6 locations. Therefore it allows the recording of any of the 6 limb leads (leads I, II, III, aVR, aVL, or aVF) plus 1 precordial lead. To represent the cardiac vector, we use quasi-orthogonal leads: D1, aVF, and V2, due to these leads are equivalent to orthogonal leads: X, Y and Z respectively (Glancy et al. 1995).

To increase the input impedance and thus reduce the effect of variations of a imperfect mechanical contact in the skin-electrode interface that causes high and unpredictable impedances that can contribute to distortion in the ECG, we use four buffer amplifiers for the signals from electrodes LA, RA, LL and V2 [Spach et al. 1966]. For the implementation of the reference input to the amplifier for the required leads, a network of 10 kΩ resistors was used to create the central terminals of Wilson for V2 lead, and of Goldberger for aVF. Definition of required leads is:

$$D1 = LA - RA \tag{1}$$

$$aVF = LL - \left(\frac{RA + LA}{2} \right) \tag{2}$$

$$V_2 = v_2 - \left(\frac{RA + LA + LL}{3} \right) \tag{3}$$

The specifications for the ECG amplifier design based in standard requirements are (Bailey et al., 1990, Association for the Advancement of Medical Instrumentation [AAMI], 1999):

- Amplifier input impedance: differential > 2.5 MΩ and common-mode > 100 MΩ
- Input range: ± 5 mV
- DC offset range: ± 300 mV
- Resolution: 10 µV
- Gain: 1000
- CMRR minimum: 80 dB
- Bandwidth: 0.05 Hz to 100 Hz

Fig. 3 shows the ECG amplifier used for a single supply operation of 5 V with a balanced AC coupled front end proposed by Spinelli et al., that has been implemented with low noise operational amplifiers TLC2274 (U2) and LMC60421 (U8).

The front end provides AC coupling for differential signals and a DC path for amplifier bias currents, which drain to ground through the RL common ECG electrode, and because the input network is not grounded, a large common mode rejection ratio (CMRR) is achieved (Spinelli et al., 2003). Because the AC coupling network is a fully differential circuit, differential and common-mode voltages define four transfer functions, so the main transfer function G_{dd} is the quotient between the Laplace transforms of the differential output voltage V_{od} and the differential input voltage V_{id} (Pallàs-Areny & Webster, 1999). Then if $R_{10}C_3 = R_{11}C_4 = \lambda_1$, and $R_{12}C_3 = R_{13}C_4 = \lambda_2$, Gdd reduces to:

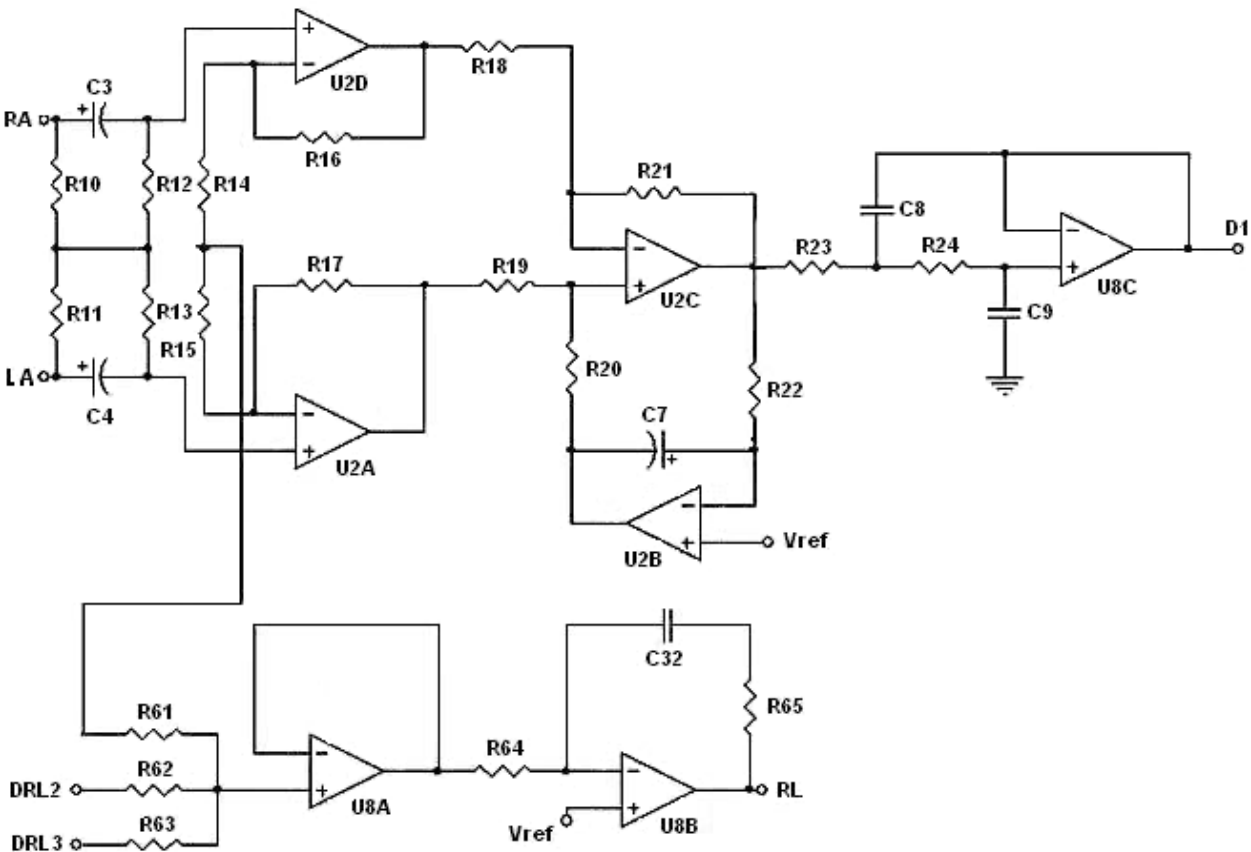Fig. 3. ECG amplifier for D1 lead

$$Gdd(s) = \frac{s\lambda_2}{1 + s\lambda_2} \qquad (4)$$

G_{dd} corresponds to a first-order high pass filter. If the time constants are not matched, the circuit has two poles and two zeros, but using passive components with a reasonable tolerance yields a transfer function similar to (4). Because G_{dd} does not depend on R_{10} and R_{11}, high values are selected in order to avoid loading effects on the input signal and also to simplify design $R_{10}=R_{11}=R_{12}=R_{13}$. Then according to AAMI standard, it is necessary an input impedance > 2.5 MΩ at 10 Hz, so $R_{10}=R_{11}=R_{12}=R_{13}$= 4.7 MΩ.

To remove input offset voltages of the op. amps, thermal noise of R_{12} and R_{13} and op-amp input voltage noise, including 1/f noise, amplifier circuit uses an integrator in a feedback loop around the difference amplifier (Pallàs-Areny & Webster, 1999). The amplifier circuit has two AC coupled stages: the front differential AC coupling network and the high pass difference amplifier, so the overall transfer function is:

$$T(s) = \frac{s\lambda_2}{(1 + s\lambda_2)} \frac{s\lambda_i A_{V0}}{(1 + s\lambda_i)} \qquad (5)$$

Where: $\lambda_i = R_{22} C_7$ and $A_{V0} = 1 + 2 R_{17}/R_{14} + R_{15}$.

The amplifier gain A_{V0} of 1001 is obtained with R_{17}= 200 kΩ and $R_{14} + R_{15}$ =400 Ω. The first factor in equation (2) corresponds to the passive AC coupling network and the second factor corresponds to the amplifier and DC restoration circuits.

Time constants λ_2 and λ_i define low frequency behavior of the amplifier and, are designed to obtain the desired transient response which is given in terms of responses to rectangular or triangular pulses. For a rectangular pulse of 1 mV amplitude and 60 ms duration, amplifier shall not produce and offset on the ECG record from the isoelectric line greater than 20 µV, so the two AC stages contribute to that offset, whose amplitude will be:

$$y(60\text{ms}) = \frac{1\text{mV}}{\lambda_2 - \lambda_i}\left[(\lambda_i - \lambda_2) + \lambda_2 e^{\frac{-60\text{ms}}{\lambda_i}} - \lambda_i e^{\frac{-60\text{ms}}{\lambda_2}}\right] \tag{6}$$

Selected values for time constants are λ_2 = 4.7 s and λ_i = 10 s that yields $y(60$ ms$)$ = 18.6 µV. From λ_2, we determine C_3 and C_4:

$$C_{3,4} = \frac{\lambda_2}{R_{12,13}} = \frac{4.7\text{s}}{4.7\text{x}10^6\,\Omega} = 1\,\mu\text{F} \tag{7}$$

From λ_i, for a proposed value for R_{22}= 10 MΩ, C_7 will be:

$$C_7 = \frac{\lambda_i}{R_{22}} = \frac{10\text{s}}{10\text{x}10^6\,\Omega} = 1\,\mu\text{F} \tag{8}$$

For bandwidth limiting in high frequency and to avoid overshoot in the amplifier response, a second order low pass filter type Sallen-Key was used. To obtain the -3 dB cutoff frequency at 100 Hz, a value of Q=0.5 for damping was selected. This value of Q corresponds to an attenuation of 6 dB at 150 Hz in the standard second order response. Therefore, in these conditions f_0=150 Hz, R_{23}=R_{24}=R, C_8=C_9=C, and proposing R=100 kΩ, then C will be:

$$C = \frac{1}{2\pi R f_0} = \frac{1}{(2\pi)(100\text{x}10^3\,\Omega)(150\text{Hz})} = 10.6 \text{ nF} \tag{9}$$

The complete transfer function with the designed time constant values results in:

$$T(s) = \frac{s4.7}{(1 + s4.7)}\frac{sA_{V0}10}{(1 + s10)}\frac{1}{(1 + s0.001)^2} \tag{10}$$

In the ECG amplifier, the voltage of the patient with respect to the amplifier's common is called the common mode voltage (V_c) that is mainly due to power line interference. Since V_c can be transformed by the amplifier into an interfering differential signal and combines with ECG, it is desirable minimize it. This voltage can be controlled by a Driven Right Leg Circuit (DRL), which uses negative feedback of common mode voltages and feeds it back to the body via the RL electrode (Winter & Webster, 1983).

In the circuit, V_c is picked up by means of averaging resistors R_{14} and R_{15} = 200 Ω, and coupled by R_{61}=10 kΩ and a buffer amplifier. After it is compared to a reference voltage (V_{REF}=V_{cc}/2), and fed back to the body with R_{64}= 10 kΩ and C_{32}= 10 nF, driving it to a V_{REF} potential. To protect the patient from amplifier faults, R_{65}= 510 kΩ limits the DC output

current of DRL circuit to 10 μA. To enable single supply operation in the ECG amplifier circuits, V_{REF}=2.5 V is connected to the noninverting input of the op-amp of the DRL (U8B) and the integrator (U2B) circuits (Spinelli et al., 2001).

2.1.2 Digitalization stage

Analog-to digital conversion parameters should be adequate to maintain fidelity criterion for visual reading of the ECG, for morphological diagnosis by digital program and for digital transmission and storage of data. To meet these requirements, a minimal sampling rate of 500 Hz with minimal resolution of 10 μV of the ECG is recommended (Bailey et al., 1990). In order to select the analog to digital Converter (ADC), it is necessary to know the characteristics of the ECG that define the required dynamic range (DR) for the ADC. The desired dynamic range for the ECG amplifier will be:

$$DR = \frac{input\ range}{resolution} = 20lg\frac{\left[+5-(-5)\right]mV}{10\mu V} = 20lg(1000) = 60\ dB \tag{11}$$

Therefore, DR for ADC must have a minimum DR of 60 dB, then the number of bits n for the ADC is:

$$n \approx \frac{DR\,(dB)}{6} \approx \frac{60}{6} \approx 10\ bits \tag{12}$$

As the system is of 4 channels (3 ECG leads and 1 for low battery voltage detection), and the sampling frequency required for each channel is 500 Hz, then we sample 4 channels at 2 kHz. The ADC that meets these requirements is incorporated into microcontroller Microchip PIC18F252, which we use to perform the control tasks of the system. This ADC is of successive approximation, it has 5 inputs multiplexed, 10-bit resolution and a conversion time of 120 μS (Microchip, 2010). The block diagram of the A/D module is shown in Figure 4, and it shows connection of each channel to the ADC, D1 is connected in AN0, aVF in AN1, V2 in AN2 and battery sensor BAT in AN3. The objective of battery sensor is to detect low voltage with a voltage divider in order to avoid errors because an inadequate recording of the ECG signals.

Digital conversion of the 4 channels is implemented by the microcontroller using the ADC module and Timer 0 (TMR0) of 16 bits. To operate the TMR0 is necessary to define some parameters. The clock used in the microcontroller is 40 MHz so that the machine cycle is equal to 0.1 μs (Microchip, 2010). If we use TMR0 without prescaler then we have a resolution of 0.1 μs. In 16-bit TMR0 overflows each 6.5535 ms, so it will be necessary to initialize TMR0 with a value to obtain the 2 ms we need, the required value is:

$$TMR0H : TMR0L = 65535 - 20000 = 45535 = 0XB1DF \tag{13}$$

Then, TMR0 registers are loaded with this value (TMR0H = 0XB1 and TMR0L = 0XDF). Subsequently microcontroller is configured to cause an interrupt whenever TMR0 overflows, in the interrupt service routine digital conversion is achieved of each channel and thus sampling frequency of 500 Hz.
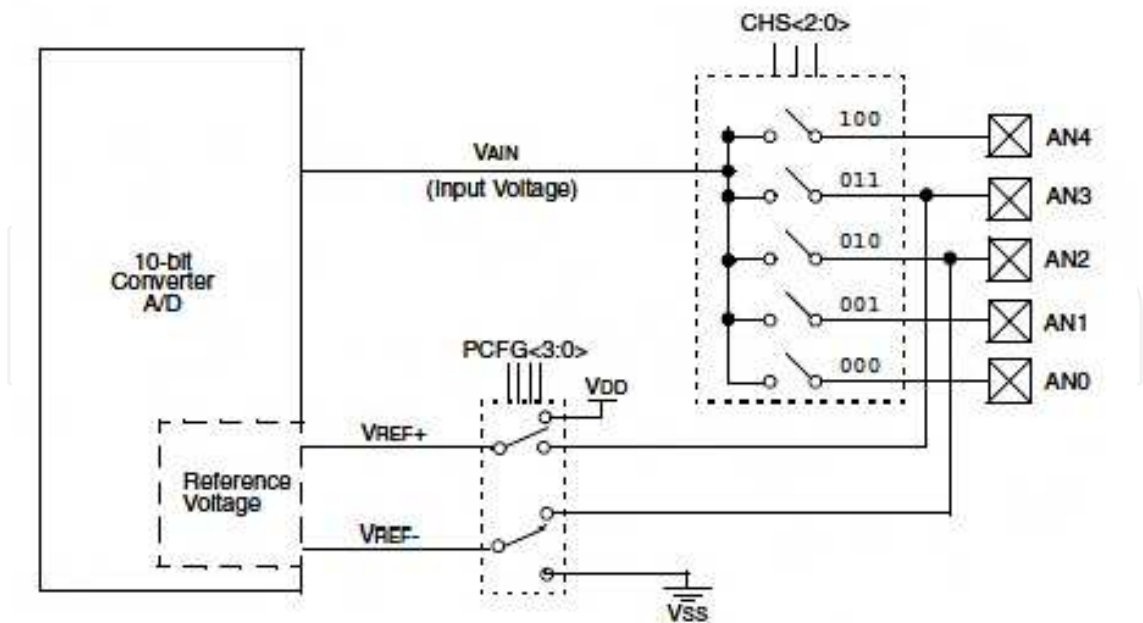
Fig. 4. A/D block diagram

2.1.3 Radiofrequency module

The device used for transmitter and receiver of the telemetry system is the nRF24L01 of Nordic Semiconductor. It is a single chip transceiver with an embedded baseband protocol engine named Enhanced ShockBurst™ (ESB), designed for ultra low power wireless applications, and for operation in the world wide Industrial-Scientific-Medical (ISM) frequency band at 2.400 - 2.4835 GHz (Nordic Semiconductor, 2007). ESB enables the implementation of ultra low power, high performance communication with low cost host microcontrollers (MCU).

The nRF24L01 is configured and operated through a Serial Peripheral Interface (SPI), in which the register map is available. The register map contains all configuration registers in the nRF24L01 and is accessible in all operation modes of the chip. The radio front end uses GFSK (Gaussian Frequency Shift Keying) modulation, and has user configurable parameters like frequency channel, output power and air data rate. Its internal voltage regulators ensure a high Power Supply Rejection Ratio (PSRR) and a wide power supply range.

2.1.3.1 Control of the nRF24L01

The nRF24L01 has a built-in state machine that controls the transitions between the different operating modes of the chip. The state machine takes input from user defined register values and internal signals. The nRF24L01 can be configured in four main modes of operation:

- Power down mode: In this configuration nRF24L01 is disabled with minimal current consumption.
- Standby modes: Standby-I mode is used to minimize average current consumption while maintaining short start up times, and part of the crystal oscillator is active. In standby-II mode extra clock buffers are active compared to standby-I mode and much more current is used compared to standby-I mode.

- Rx mode: In this mode the receiver demodulates the signals from the RF channel, constantly presenting the demodulated data to the baseband protocol engine, which constantly searches for a valid packet.
- Tx mode: In this mode the device transmits a data packet previously loaded by the control stage (MCU).

Transmitter and receiver are programmed with the same RF channel frequency and the same air data rate to be able to communicate with each other. Then, a RF channel frequency of 2.4 GHz, a bandwidth of 2 MHz and an air data rate of 2 Mbps were used. This air data rate provides lower average current consumption and reduced probability of on-air collisions. The PA control was used to set the output power from the nRF24L01 power amplifier (PA) to 0 dBm with a DC current consumption of 11.3 mA. In the nRF24L01 receiver the gain in the Low Noise Amplifier (LNA) is controlled by the LNA gain setting, which it is possible to reduce the current consumption in RX mode with 0.8 mA at the cost of 1.5 dB reduction in receiver sensitivity.

2.1.3.2 Communication protocol

The embedded baseband protocol engine (ESB) is based on packet communication and supports various modes from manual operation to advanced autonomous protocol operation, which it is a desired characteristic in this application. It has internal FIFOs registers that ensure a smooth data flow between the radio front end and the system's MCU, so it reduces system cost by handling all the high-speed link layer operations, and firmware and required memory in the MCU. The format of the ESB packet contains a preamble field, address field, packet control field, payload field and a cyclic redundancy check (CRC) field (Figure 5).

Fig. 5. Format of the Enhanced ShockBurst™ (ESB) packet

- Preamble: The preamble is a bit sequence used to detect 0 and 1 levels in the receiver. The preamble is one byte long and is either 01010101 or 10101010. If the first bit in the address is 1 the preamble is automatically set to 10101010 and if the first bit is 0 the preamble is automatically set to 01010101. This is done to ensure there are enough transitions in the preamble to stabilize the receiver.
- Address: In this field address for the receiver is defined, and ensures that the correct packet are detected by the receiver. The address field can be configured to be 3, 4 or, 5 bytes long.
- Packet Control Field: This field consists of 9 bits. The most significant 6 bits are used to specify the size in bytes of the data field, which can be from 0 to 32 bytes. The 2 bit PID (Packet Identity) field is used to detect if the received packet is new or retransmitted, this prevents the MCU receives the package more than once. The PID field is incremented at the TX side for each new packet received through the SPI. The PID and CRC fields are used by the PRX device to determine if a packet is retransmitted or new. The last least significant bit is used for a special feature of the nRF24L01 called auto acknowledgement.

- Data: This field is the user defined content of the packet. It can be 0 to 32 bytes wide and is transmitted on-air as it is uploaded (unmodified) to the device.
- CRC: This field is used as the error detection mechanism in the packet. It may either be 1 or 2 bytes and its calculation is based on the contents of the fields of address, Packet Control Field, and Data. No packet is accepted by ESB if the CRC fails. The polynomial for 1 byte CRC is $X8 + X2 + X + 1$. The polynomial for 2 byte CRC is $X16 + X12 + X5 + 1$.

ESB provides automatic packet handling and timing. In transmission, ESB assembles the packet and clocks the bits in the data packet into the transmitter for transmission. In reception, ESB constantly searches for a valid address in the demodulated signal. When ESB finds a valid address, it processes the rest of the packet and validates the packet by CRC. If the packet is valid the payload is moved into the RX FIFO. The high speed bit handling and timing is controlled by ESB.

2.1.3.3 Data and control interface

The data and control interface gives access to all the features in the nRF24L01. The data and control interface consists of the following six 5 V tolerant digital signals:
- IRQ: this signal is active low and is controlled by three maskable interrupt sources
- CE: this signal is active high and is used to activate the chip in RX or TX mode
- CSN: SPI enable signal
- SCK: SPI clock signal
- MOSI: SPI serial data input signal
- MISO: SPI serial data output signal

The SPI is a standard SPI with a maximum data rate of 8 Mbps. In this application, IRQ pin is used mainly to carry out the monitoring of device.

2.1.3.4 nRF24L01 transceiver circuit

The complete nRF24L01 transceiver circuit of 2.4 GHz with the recommended components according to the manufacturer's data sheet is shown in Figure 6 (Nordic Semiconductor, 2007). The ANT1 and ANT2 output pins provide a balanced RF output to the antenna. The pins must have a DC path to VDD_PA, through a RF choke, and a recommended matching network for 50 Ω load impedance is used in the circuit. To achieve a crystal oscillator solution with low power consumption and fast start-up time a crystal with a low load capacitance specification C_L must be used (typically 12 pF), and also with a lower equivalent parallel capacitance C_0 (typically $C_0=1.5pF$), but may increase the cost of the crystal.

With respect to PCB layout of the circuit is necessary a good design to achieve good RF performance.

A PCB with a minimum of two layers including a ground plane is recommended for optimum performance. The nRF24L01 DC supply voltage should be decoupled as close as possible to the VDD pins with high performance RF capacitors, and it should be filtered and routed separately from the supply voltages of any digital circuitry. Long power supply lines on the PCB should be avoided. Full swing digital data or control signals should not be routed close to the crystal or the power supply lines. A fully qualified RF-layout for the nRF24L01 and its surrounding components, including matching networks, is given by the manufacturer (Nordic Semiconductor, 2007).
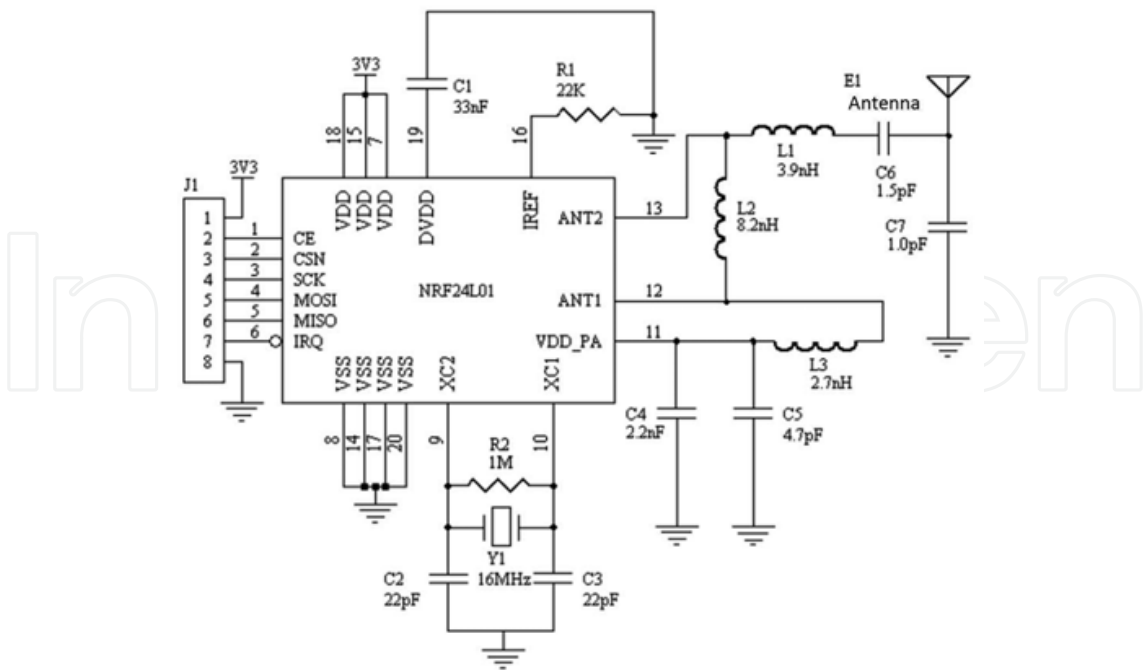
Fig. 6. nRF24L01 transceiver circuit with single ended 50 Ω RF output

2.1.4 Control unit

The control unit is the most important part of the transmitter, because this unit receives data of digitized ECG, battery monitoring and transmission and reception via radio frequency. To perform these tasks a microcontroller Microchip PIC18F252 with RISC architecture was used. Figure 7 shows the PIC18F252 connected to all its peripherals.
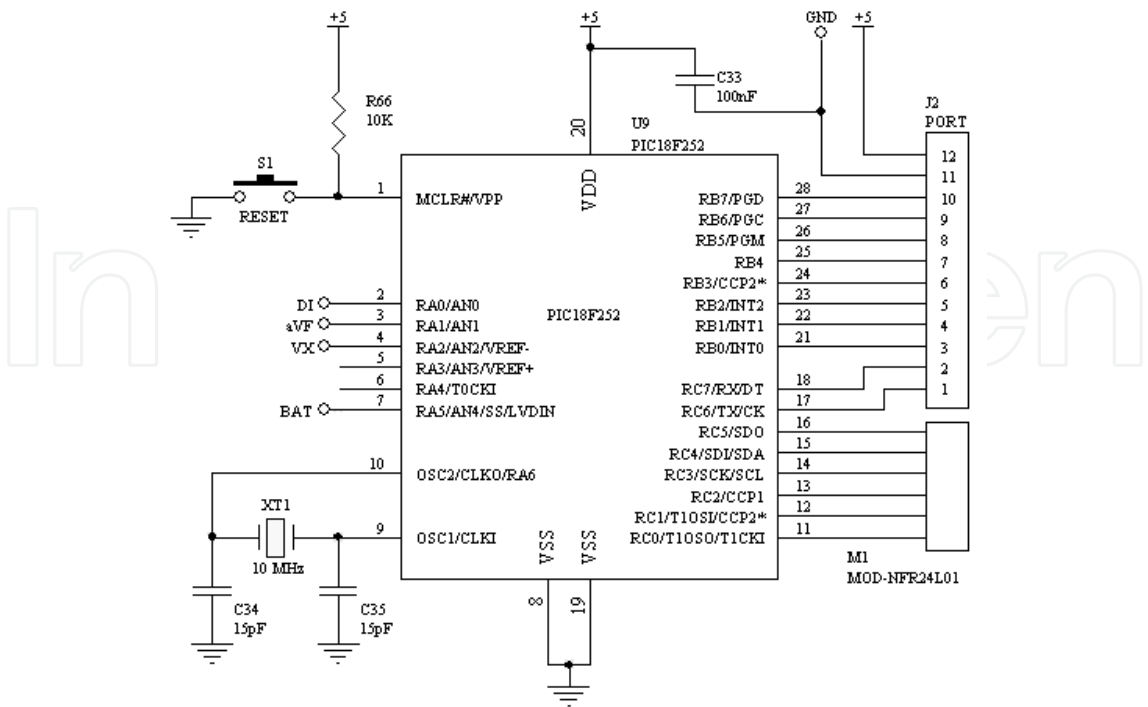

Fig. 7. PIC18F252 as main controller of the transmitter

The MCU operates at a speed of 10 MIPs with a 10 MHz crystal and the PLL (Phase-Locked Loop) enabled. Analog signals from DI, aVF, Vx and BAT are digitized by the internal ADC, in where the TMR0 sets the sampling rate and the conversion is controlled by TMR0 interrupt. Once digitized the signals are sent to nRF24L01 through the SPI port, where the control of all radio functions are performed. The RB7 pin of the port B is used only to show system status through a LED. The port B is reserved for future expansions, being able to connect an optional SD memory card, LCD screen etc. The MCLR pin is used for MCU Reset and for development purposes only.

The figure 8 shows the flowchart of the algorithm implemented in the firmware of the PIC18F252. The language used for development is the C compiler using MPLAB C Compiler for PIC18 MCUs in professional version 3.00, and the development environment is the MPLAB version 8.00 both of Microchip, Inc.
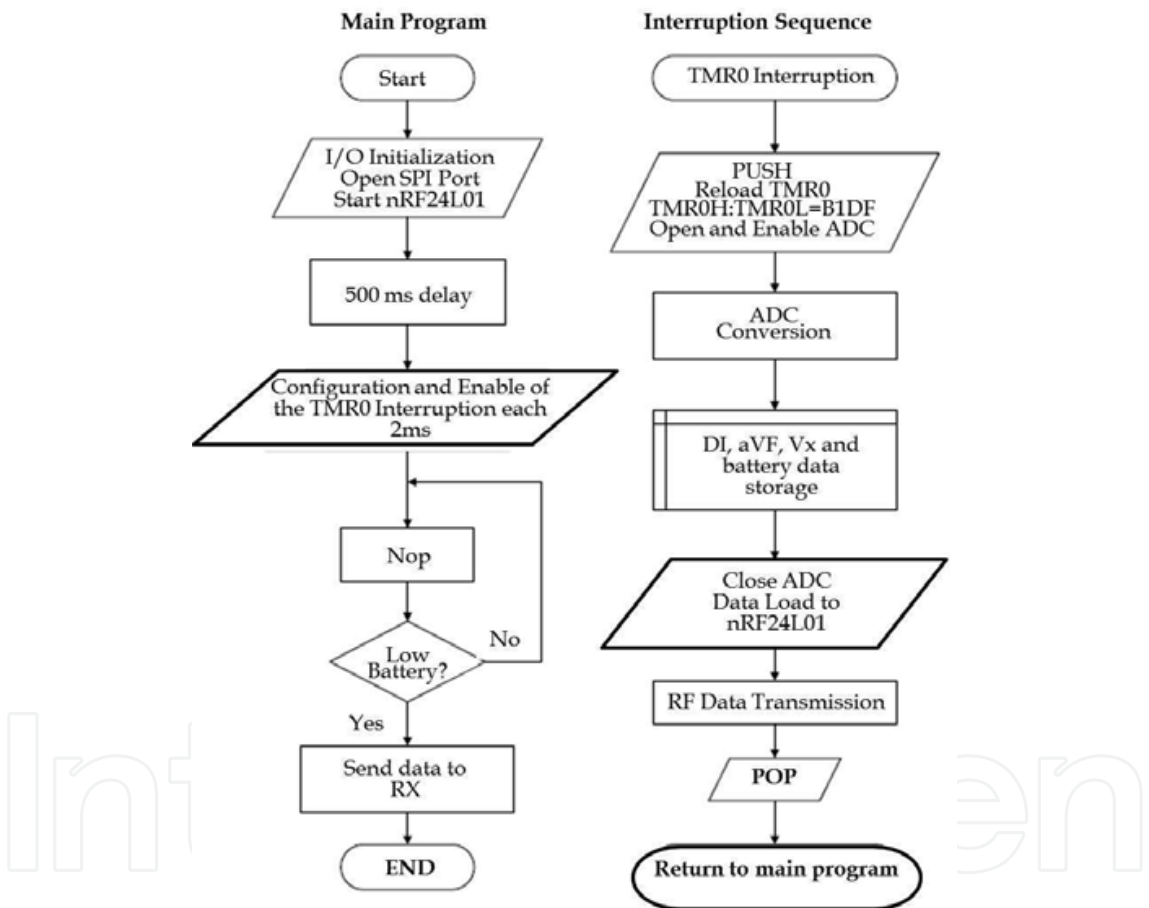
Fig. 8. Flowchart of the algorithm implemented in the PIC18F252 firmware as transmitter

2.1.5 Power supply

The general characteristics required of the power supply are:
- Supply with type AA batteries
- Regulated voltage outputs of ± 5 V and 5 V
- Maximum current of 100 mA
- Low ripple
- High efficiency

As first stage of the power supply, the high efficiency step-up DC to DC converter NCP1400 is used to generate a regulated voltage of 5 V with 100 mA of output current to generate a voltage of -5 V from a +5 V a switched capacitor voltage inverter MAX828 is used which has high efficiency and low operating current. To obtain the reference voltage of 2.5 V required to shift ECG baseline and the matching with ADC range of 0 to 5 V, a micropower voltage reference diode LM385 is used which provides a current of 15 µA to 20 mA with a resistor of 200 kΩ.

2.2 Receiver
The block diagram is shown in the figure 2b, and it is composed of a control unit, a RF module, two communication ports and a power supply.

2.2.1 Radiofrequency module
The design of this section is identical to the RF transmitter module but now the transceiver is configured as receiver. Due to both modules use the same MCU, driver that is used in the firmware of both modules is the same. At the reception, data are received first in the lowest layer referring to the protocol explained previously and inversely on the transmission (Fig. 5). Unpacked data are put into the internal registers of the microcontroller to be processed later. The electric circuit is also identical to the transmitter (Fig. 6).

2.2.2 Control unit
To perform all tasks in this stage, the same PIC18F252 microcontroller is used. Connection of the PIC18F252 with its peripherals is shown in Figure 9. The PIC18F252 has connected in pin MCLR a push button to reset if it is necessary and for development purposes, in pins RA0, RA1 and RA2, three LEDs for general indication of the system status (red = power, green = reception and orange = transmission), a 10 MHz crystal for MCU clock, the RF module connected to the port SPI and in the UART lines (RX and TX) the interface RS232 formed by integrated circuit MAX232 necessary to match voltage levels or the USB controller only one at a time.
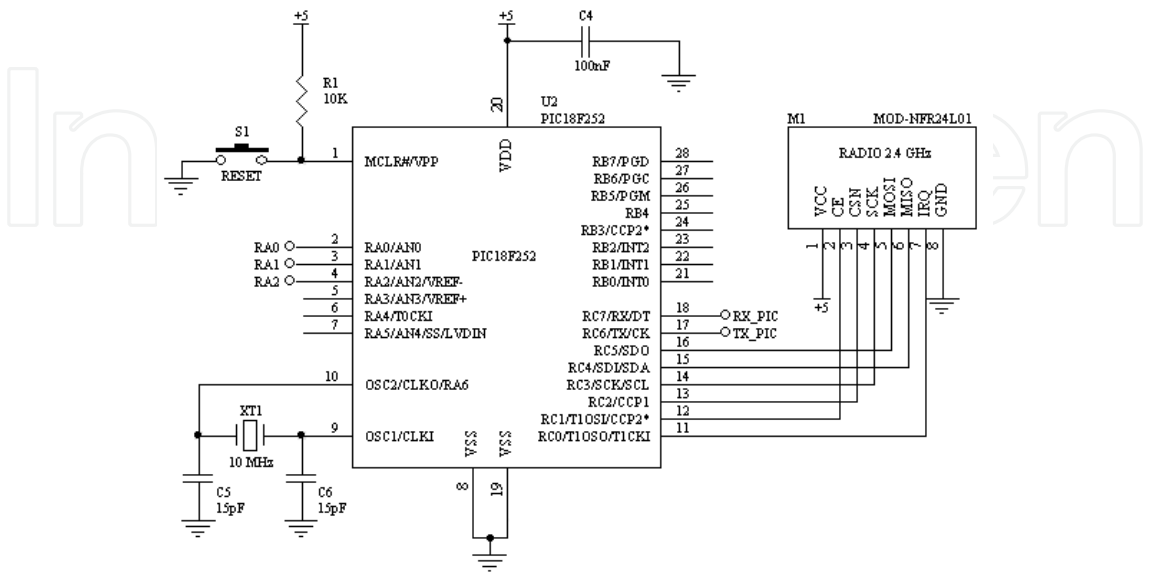

Fig. 9. PIC18F252 as main controller of the receiver

The PIC18F252 firmware is also written in C using the compiler MPLAB C Compiler for PIC18 MCUs in its professional version 3.00 and the development environment is the MPLAB version 8.00 both of Microchip, Inc. In the figure 10 shows the flowchart of the algorithm implemented in the firmware of the PIC18F252.
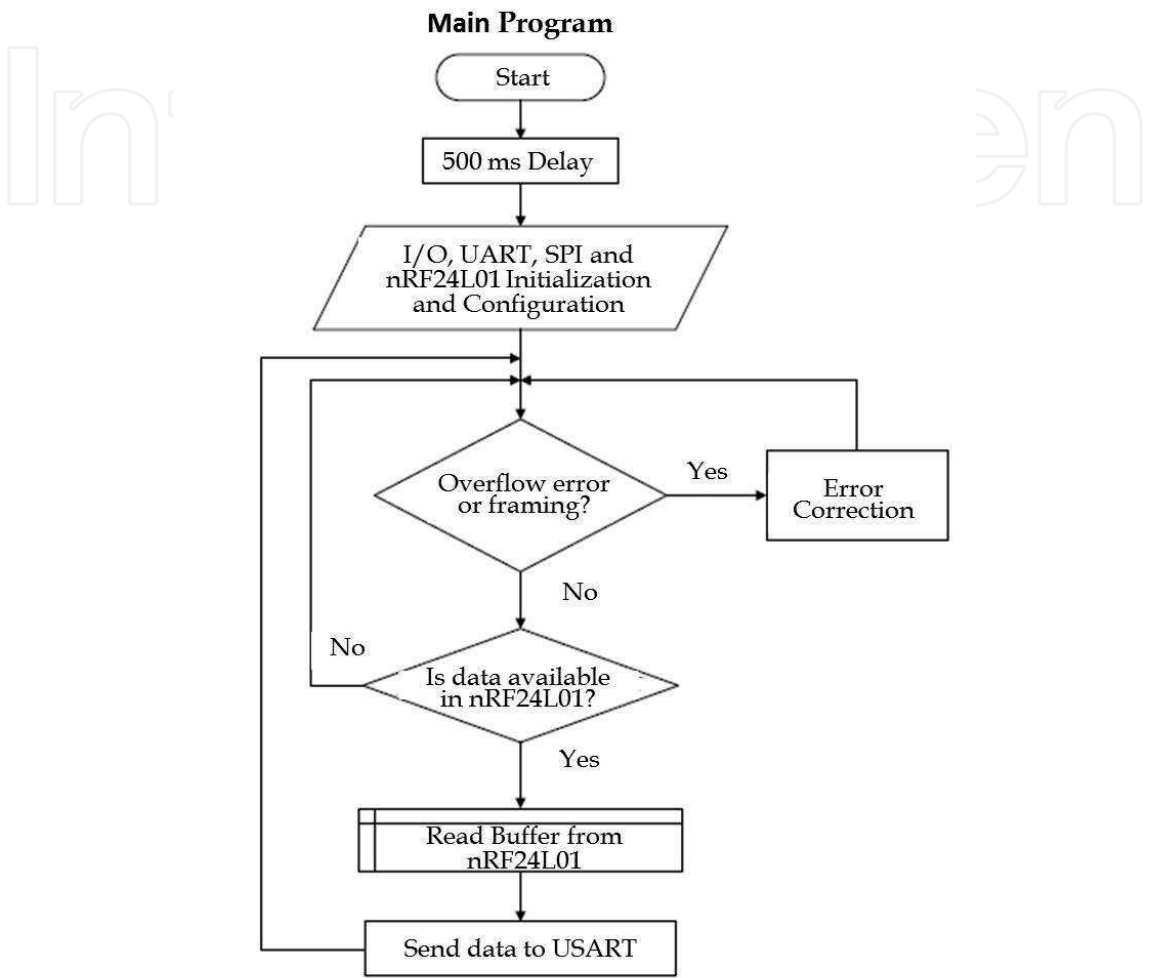

Fig. 10. Flowchart of the algorithm implemented in the PIC18F252 firmware as receiver

2.2.3 RS-232C Interface
The communications port uses the USART interface of PIC18F252. The configuration and control of USART is performed by the MCU firmware. The device used that conditions MCU and RS-232C voltage levels is the MAX232. MCU and computer must be configured to operate to 115,200 Bauds, without parity, 8 bits data and 1 bit stop. A power supply with a regulated voltage of 5 V is used in this interface.

2.2.4 Acquisition, display, storage, conditioning and processing of data
The format used to transmit the packet of each digitized sample to the RS-232C interface is shown in figure 11. The data are sent in hexadecimal and each parameter consists of 1 byte if we use ADC in 8-bit mode, and 2 bytes if we use the maximum 10 bit allowed for the digitization of each sample.

| Header | DI Data | aVF Data | Vx Data | Battery Information |

Fig. 11. Format of the data packet sent by the receiver to the RS-232 interface

The software implementation of this equipment was performed in LabVIEW®. The software purposes are the acquisition, display and storage of data, and the development of an R wave peak detection algorithm. In order to achieve these objectives different sub-VIs gathered together into two different main VIs were realized. The general structure of the first program (Acquisition VI) is described in Figure 12.
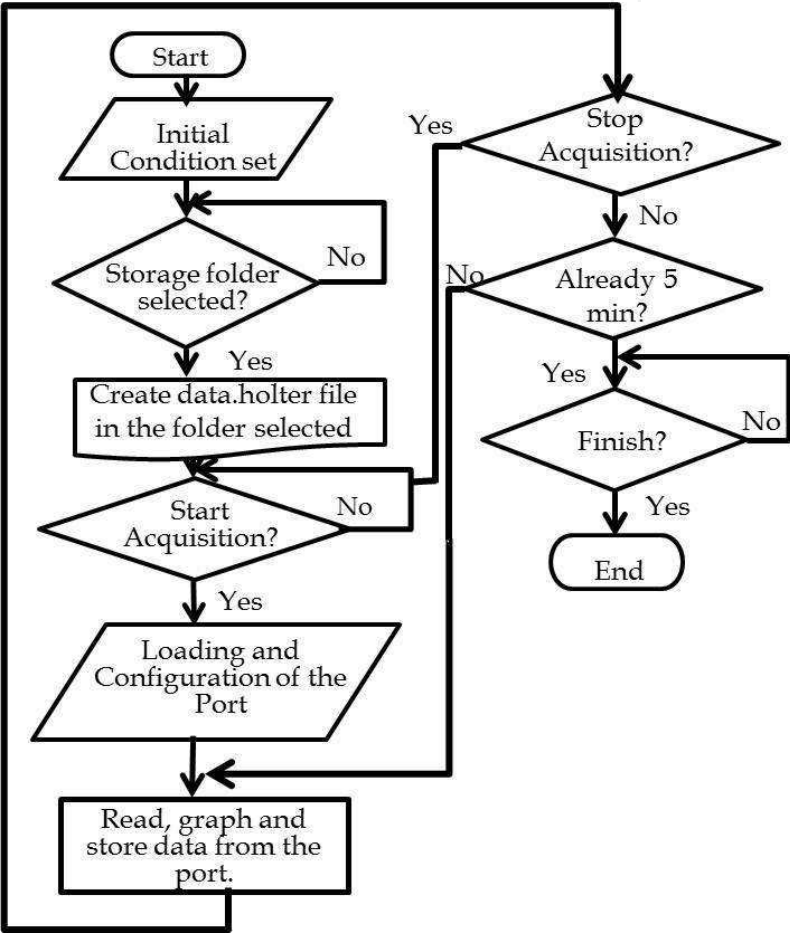
Fig. 12. General block diagram for acquisition VI

In this VI is where the acquisition of data is realized. As shown in the preview diagram when the VI starts, initial conditions as the position of frontal panel (FP) (Fig. 13) and button initialization are implemented. Then the user must select a folder in the CPU in order to continue. Once selected the folder where the data will be stored the program automatically generates appropriate files for the signal storage. At this point, user must indicate at which port is connected the equipment and ensure the configuration in the CPU is the correct one. Start acquisition's button will be available after this and the user will define when to start the acquisition. When the initial button is pressed the acquisition process starts during 5 minutes. There is also the option of stopping the acquisition process in this stage by pressing

the stop button. Until the acquisition process is finished, exit button is allowed. At this phase user can choose between two options. One is to start a new acquisition overwriting previewed data acquired. Or user can choose to finish the acquisition VI program.

Fig. 13. Acquisition VI program frontal panel

Then the program automatically starts the second VI (conditioning VI) where the signal previously acquired will be processed. General structure of the conditioning VI is shown in Figure 14. When this VI starts it sets the initial conditions for the graphs charts, the buttons, and the FP position. The VI knows where the data was previously stored, so when the user presses the start button it automatically starts to takeoff from the original signal the trend, the noise and it process this information to obtain the R wave peak detection.

Detrending process performed in this VI is implemented with the LabVIEW® Wavelet Analysis Detrend VI. It considers the energy in the ECG signal to remove baseline wander due to low frequency artifacts (Weng et al., 2006). The denoising process is realized with the Wavelet Analysis Denoise VI. This VI performs noise reduction using the undecimated wavelet transform (UWT) for the elimination of high-frequency component due to noise.

At the end, the R wave peak detection is performed using a self-programmed variation of the LabVIEW® Wavelet Analysis Multiscale Peak Detection. This variation allowed the program a complete and correct detection of all the R wave peaks in the ECG signal. Figure 15 shows the final FP of the conditioning VI.
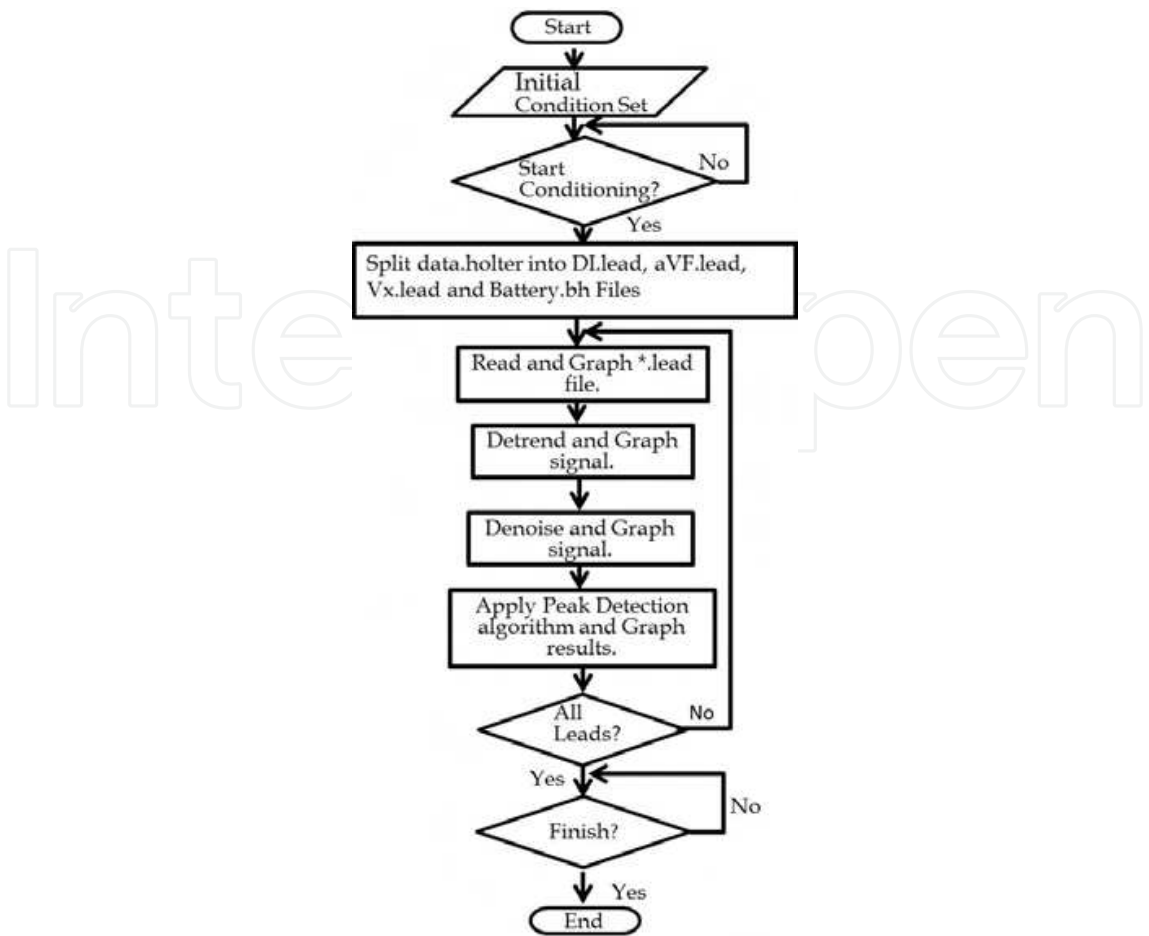
Fig. 14. General block diagram for conditioning VI

Fig. 15. Conditioning VI frontal panel after complete R wave peak detection

The programming process of both VI was realized with Queued State Machine-Producer Consumer architecture (QSM-PC). This architecture is used for event structures that send commands for asynchronous processes. The different tasks inside the VI (e.g. initializations, acquisition, and storage) are the consumers or commands handler in the QSM-PC. These commands are triggered by events or producers (e.g. button pressing, status changes, and user's actions) which controls the states of the QSM-PC. These states can be sequentially assigned by the programmer in order to achieve certain structure (Fig. 16).

Fig. 16. Queued State Machine-Producer Consumer architecture used for the VI's programming

The acquisition VI program consists of 6 commands handlers and three producers (Fig. 17).
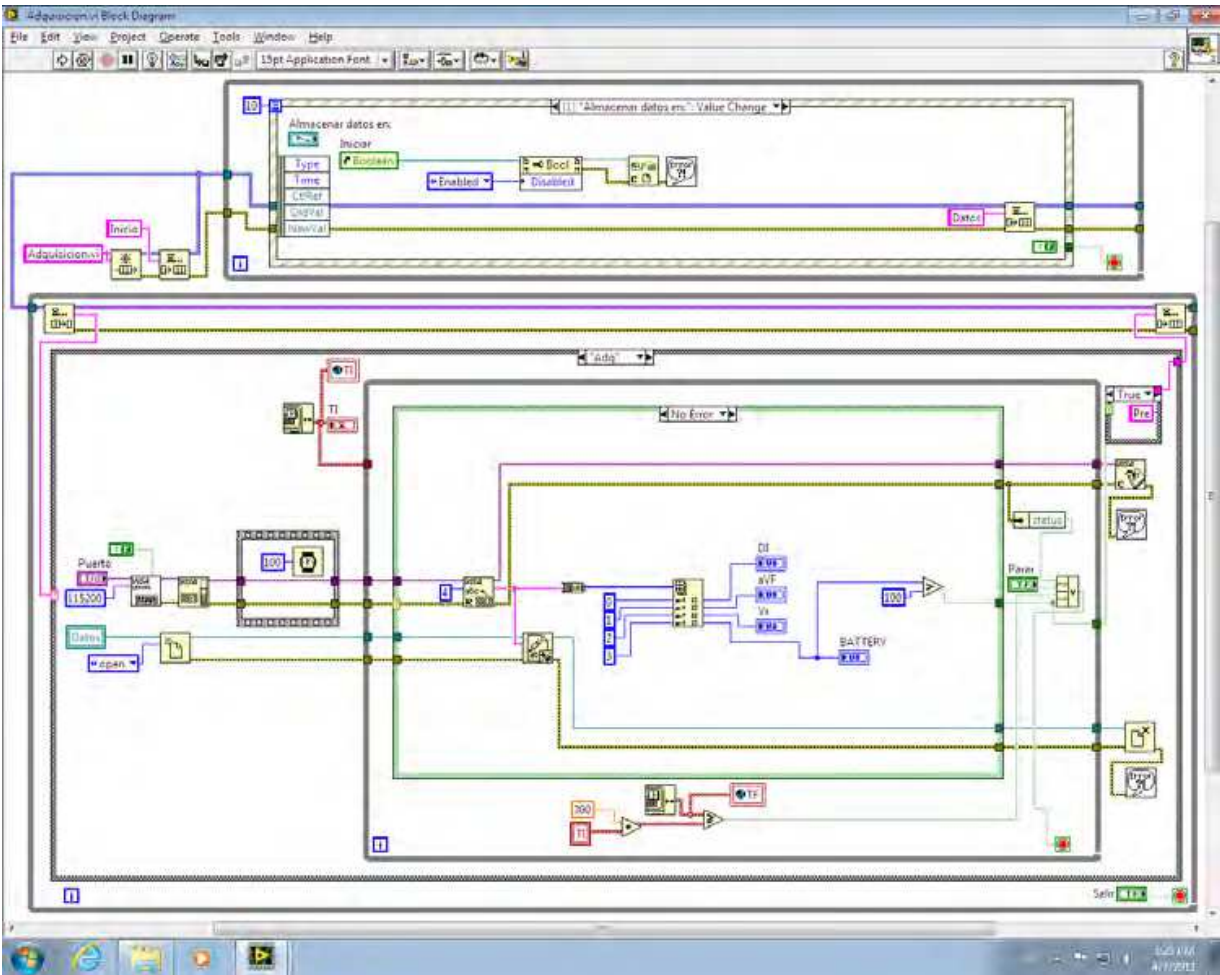
Fig. 17. Diagram block of the acquisition VI in acquisition's handler and path's change value producer

The first command handler is the one that sets all the initial condition such as button conditions, window position, path conditions and the graphs initial set. The second handler is to create the file where data will be saved. The next handler is a pre-setting for showing the data while it is obtained and after this the acquisition handler begins. Once finished the acquisition the next handler is in charge of setting initial conditions again for a new acquisition or the end of the program. At least all programs must have a default handler. This handler is just a loop in the program that waits for a producer to be triggered. For the producers as stated before there are three. One is for the path's change value event that assures the place where data will be stored. The second producer is for the beginning of data acquisition. This producer is triggered by pressing the start button. At least, the third producer is for exiting the program. This occurs when the Finish button is pressed.

Figure 18 shows the Conditioning VI which consists of 6 commands handlers and two event producers. Just as the first VI, the first handler implements the initial conditions. The second handler is pre-setting condition where data is arranged. This arranging is made by a sub-VI constructed for decoding the data previously acquired and stored. After this the conditioning handler starts.
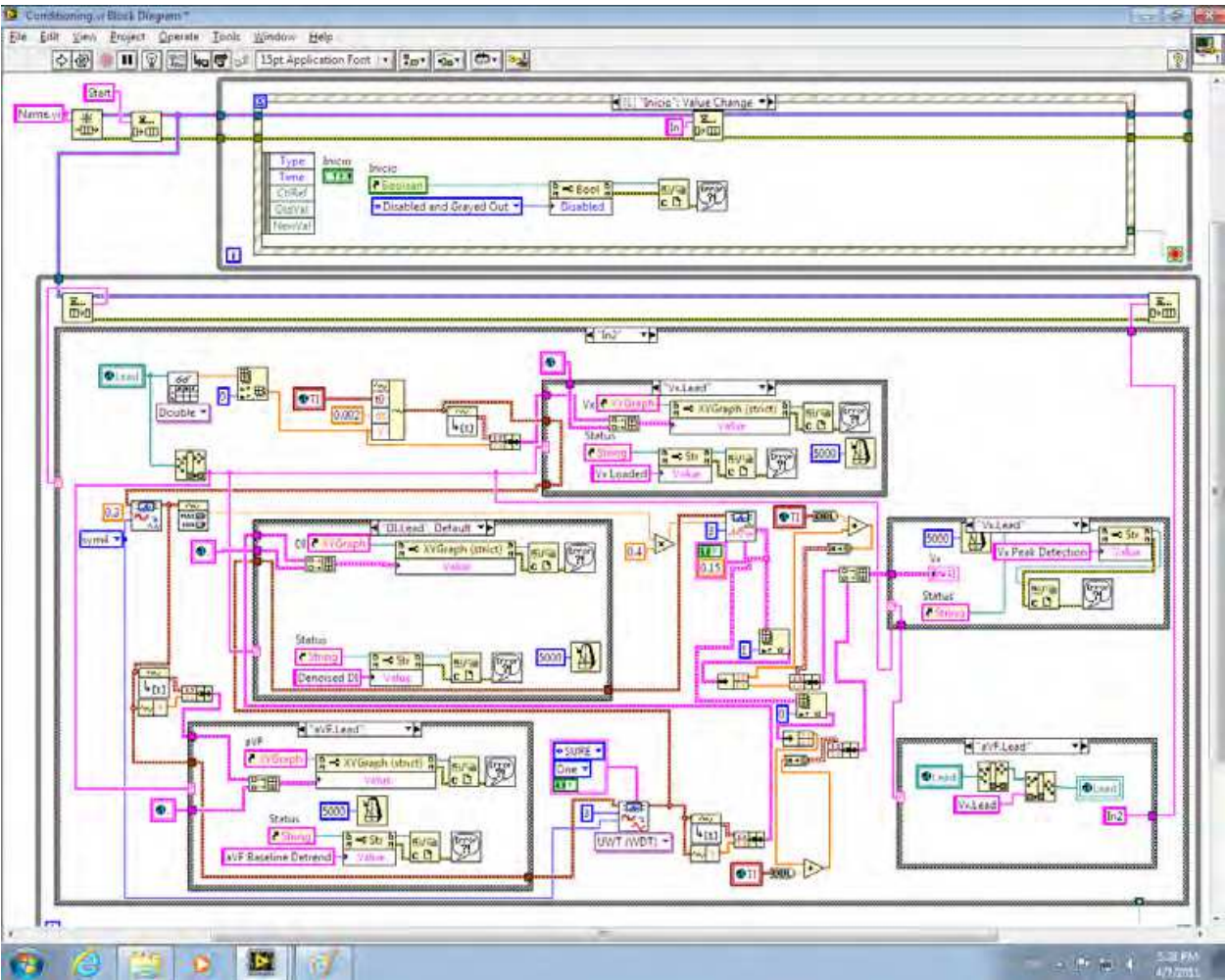

Fig. 18. Diagram block of the conditioning program in the conditioning handler and the start event producer

This handler has inside a sub-VI in which the detrending, denoising, and peaks detection are integrated. Then after conditioning is finished, the next handler is the post-conditioning. This handler configures a display alarm indicating that the conditioning is finished. At least there is an exit handler that finishes the program. This program also has a default handler that waits for an event's producer action. The event producers for this program are just two. One is for beginning the conditioning, and the other for finishing the program.

3. Results

To quantify the rejection of common mode interferences of the ECG amplifiers, we measured its Common Mode Rejection Ratio (CMRR), which is the quotient between the differential mode gain Ad and the common mode gain Ac, and it can be expressed in decibels where CMRR (dB)=20 lg (Ad/Ac). Initially, we measured the frequency response of the differential gain with one input of ECG amplifier grounded, and later, the common mode gain with both inputs of ECG amplifier short-circuited. Obtained values were: Ad= 1000, bandwidth=0.05 to 100 Hz and CMRR of 88 dB at 60 Hz with a mean of 84 dB in all bandwidth. Similar results were obtained in the other two amplifiers. Figure 19 shows the frequency response of the Ad and CMRR of the ECG amplifier.

With respect to the maximum value of DC voltage that ECG amplifier can tolerate in its input, the measured value was of ± 500 mV.

(a)

(b)
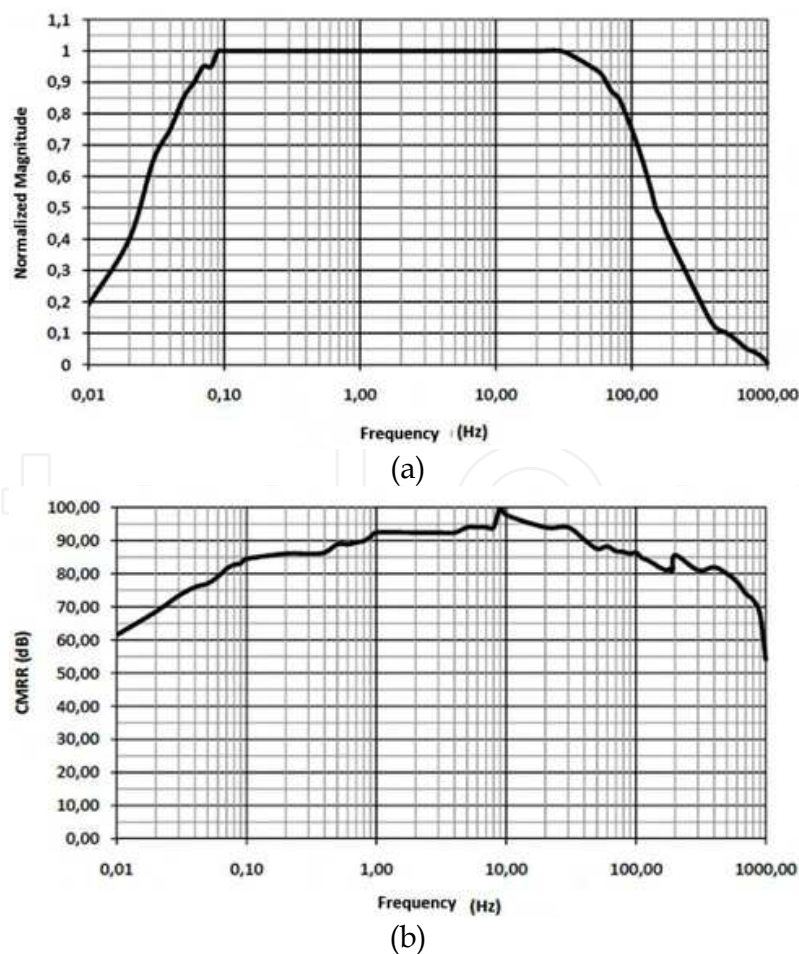
Fig. 19. Frequency response of ECG amplifier (a) Ad. (b) CMRR.

As power supply for the system, two AA rechargeable batteries of 2500 mAh were used to provide power to all circuits of the transmitter at 0 dBm output power. The maximum current consumption under normal operation was of 115 mA with a battery life-time minimum of 24 hours as required. To measure the distance of the RF link of the whole system, we tested the system in different sites using the maximum power of RF transmitter module at 0 dBm with a small ceramic chip antenna resulting from 10 m in indoors and 30 m in outdoors.

One of the developed applications implemented in LabVIEW® analyzes the variations in the RR intervals named HRV, using statistics methods with a record of 24 hours of the RR series (Fig. 20). The first stage covers the elimination of artifacts within the RR series; these are caused by the omission of R waves or the detection of nonexistent R waves (Fig. 21). In the second stage, statistics indexes are calculated and grouped in 5 minutes records according to standards of measurement of HRV (Task Force of the European Society of Cardiology and the North American Society of Pacing and Electrophysiology, 1996). The third stage reports 7 statistics indexes accompanied of a histogram (Fig. 22).
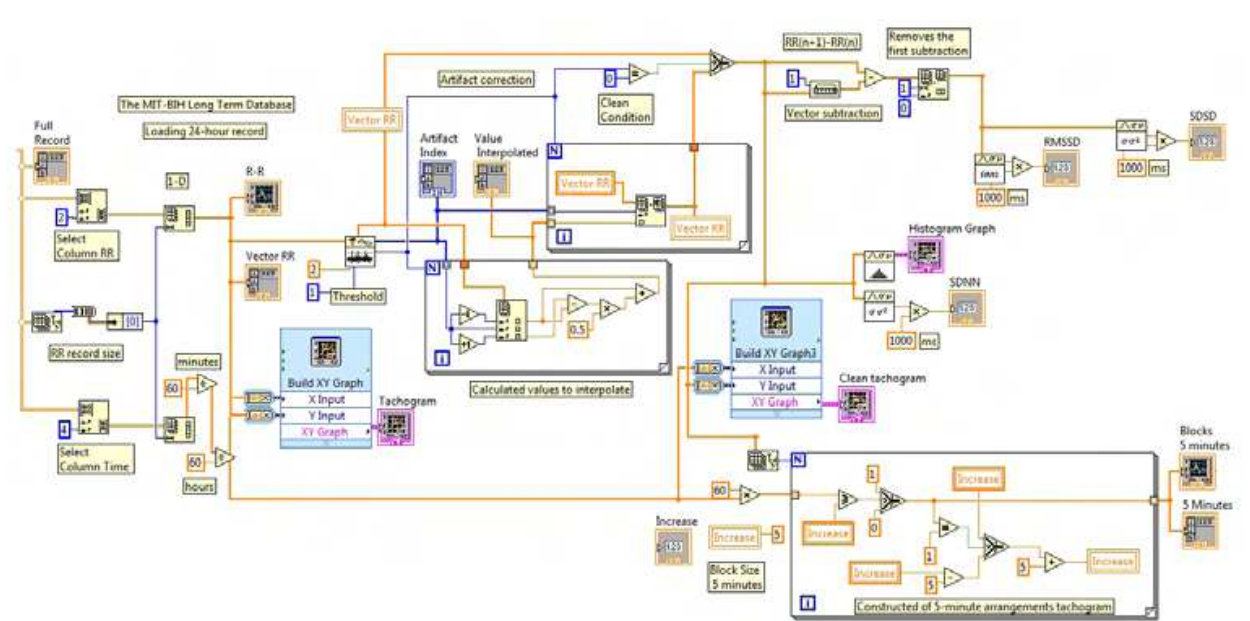

Fig. 20. Elimination of artefacts and segmentation of the record in blocks of 5 minutes
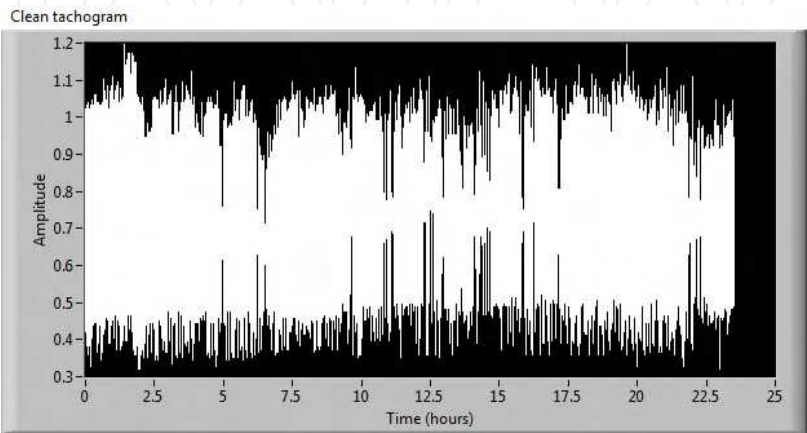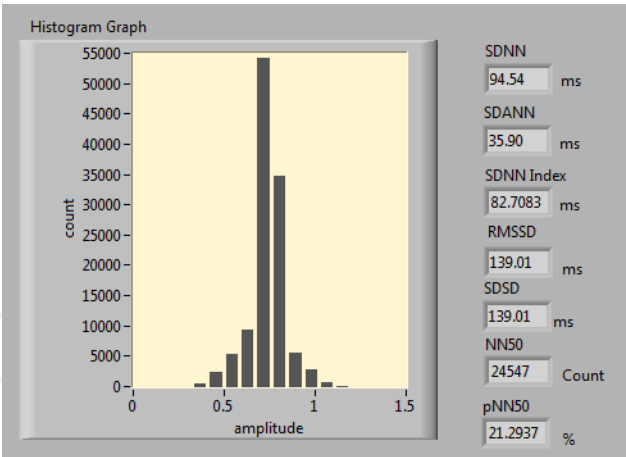

Fig. 21. Clean tachogram

Fig. 22. Histogram and statistics indexes.

The printed circuit boards of the transmitter and receiver are shown in figure 23. Dimensions of the system are: transmitter (11 cm x 14 cm x 4 cm), receiver (8 cm x 7.5 cm x 3 cm). The telemetry ambulatory system is shown in figure 24.
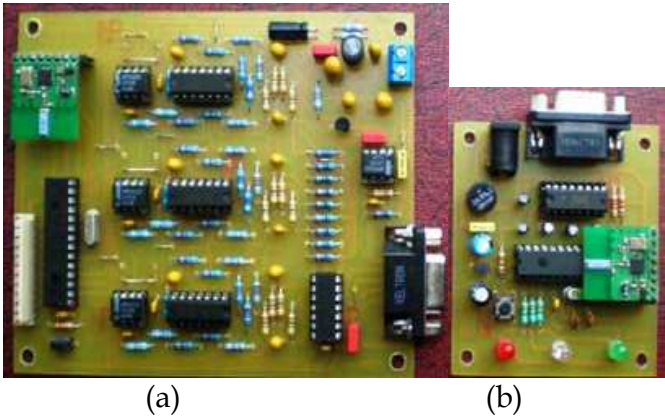

(a)   (b)

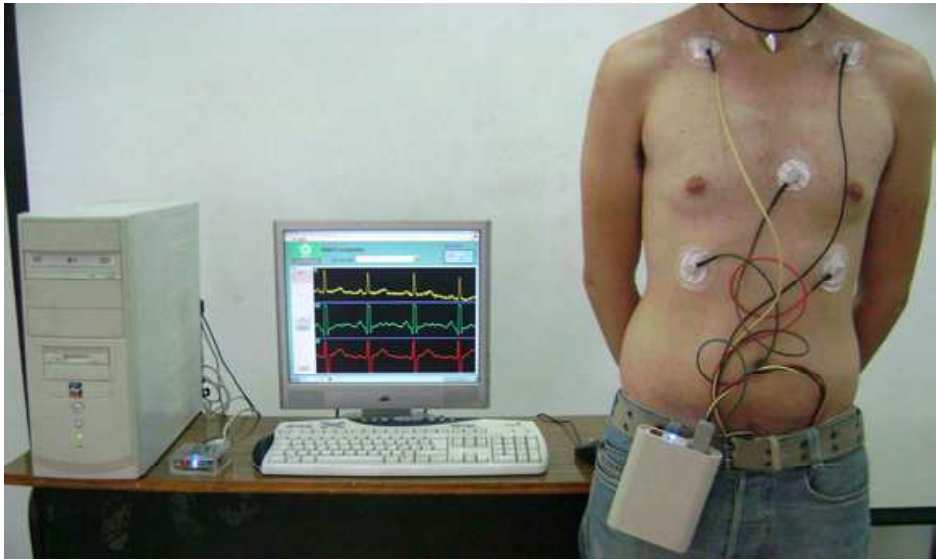Fig. 23. Printed circuit boards (a) Transmitter. (b) Receiver.

Fig. 24. Telemetry ambulatory system

4. Conclusion

The prototype of ECG telemetry ambulatory system developed fulfills the requirements of real time transmission of long term records, low power consumption and low cost. In agreement with standard requirements to ensure accurate diagnosis, ECG amplifiers meet important features of input impedance, input range, DC offset range, resolution, gain, CMRR, bandwidth, reduction of movement artifacts and baseline drift, and ADC with sampling frequency and resolution.

With respect to digital stage of the system, high integration in transmitter and receiver is achieved using two integrated circuits, a microcontroller and a RF transceiver. RF communication is robust to electromagnetic interferences and with low probability of error due to the communication protocol used. Software for implementation of acquisition, display and storage of the 4 signals (3 ECG leads and battery voltage), detection of R wave peak of ECG and processing of R-R intervals based in LabVIEW® was developed for the study of heart rate dynamics.

This system will be used to create a database of long-term records of normal subjects and patients that it will allow the clinical research of new indexes to assess risk of malignant ventricular arrhythmias, and analyse dynamics of other important electrophysiological variables like ST segment changes, QT interval (duration and dispersion) and T-wave alternans. Future work will be performed to reduce the size of the transmitter using surface mount devices.

5. References

Association for the Advancement of Medical Instrumentation (AAMI). (1999). *American National Standard ANSI/AAMI EC38:1998, Ambulatory Electrocardiographs*, AAMI, ISBN 1-57020-115-3, Arlington, VA

Bailey, J.J., Berson, A.S., Garson Jr., A., Horan, L.G., Macfarlane, P.W., Mortara, D.W., & Zywietz, C. (1990). Recommendations for standardization and specifications in automated electrocardiography: bandwidth and digital signal processing. A report for health professionals by an ad hoc writing group of the Committee on Electrocardiography and Cardiac Electrophysiology of the Council on Clinical Cardiology, American Heart Association. *Circulation*, Vol. 81, No. 2, (February 1990), pp. 730-739, ISSN 1524-4539

Daskalov, I., Christov, I., & Dotsinsky, I. (1997). Low frequency distortion of the electrocardiogram. *Med. Eng. Phys.*, Vol. 19, No. 4, (June 1997), pp. 387-393, ISSN 1350-4533

Fuster, V. (2002). Investigación cardiológica aplicada. Retos en el nuevo milenio. *Revista Española de Cardiología*, Vol. 55, No. 4, (Abril 2002), pp. 327-332

Glancy, J.M., Garratt, C.J., Woods, K.L. & De Bono, D.P. (1995). Three-lead measurement of QTc dispersion. *J. Cardiovasc. Electrophysiol.*, Vol. 6, No. 11, (November 1995), pp. 987-992

Goldberger, J.J., Cain, M.E., Hohnloser, S.H., Kadish, A.H., Knight, B.P., Lauer, M.S., Maron, B.J., Page, R.L., Passman, R., Siscovick, D., Stevenson, W.G. & Zipes, D.P. (2008). American Heart Association/American College of Cardiology Foundation/Heart Rhythm Society scientific statement on noninvasive risk stratification techniques for identifying patients at risk for sudden cardiac death: a scientific statement from

the American Heart Association Council on Clinical Cardiology Committee on Electrocardiography and Arrhythmias and Council on Epidemiology and Prevention. *Circulation*, Vol. 118, No. 14, (September 2008), pp. 1497–1518, ISSN 1524-4539

Instituto Nacional de Estadística, Geografía e Informática (INEGI). (April 2010). Defunciones generales totales por principales causas de mortalidad 2008, In: *Estadística, Demografía y Población, Mortalidad, Causas de defunción,* 03.03.2011, Available from: http://www.inegi.org.mx/sistemas/sisept/Default.aspx?t=mdemo107&s=est&c=2 3587

Kadish, A.H., Buxton, A.E., Kennedy, H.L., Knight, B.P., Mason, J.W., Schuger, C.D. & Tracy, C.M. (2001). ACC/AHA clinical competence statement on electrocardiography and ambulatory electrocardiography: a report of the American College of Cardiology/American Heart Association/American College of Physicians-American Society of Internal Medicine Task Force on Clinical Competence (ACC/AHA Committee to Develop a Clinical Competence Statement on Electrocardiography and Ambulatory Electrocardiography). *Circulation*, Vol. 104, No. 25, (December 2001), pp. 3169–3178, ISSN 1524-4539

Kennedy, H.L. (2004). Use of long-term (Holter) electrocardiographic recordings, In: *Cardiac Electrophysiology: From Cell to Bedside*, Zipes D.P., Jalife J., pp. 772-787, Saunders, ISBN 0721603238, Philadelphia, USA

Metha, D., Curwin, J., Gomes, J.A. & Fuster, V. (1997). Sudden death in coronary artery disease: acute ischemia versus myocardial substrate. *Circulation*, Vol. 96, No. 9, (November 1997), pp. 3215–3223

Microchip. (November 2010). PIC18FXX2 Datasheet, In: *Home, Products, 8-bit PIC® Microcontrollers*, 10.11.2010, Available from:
http://www.microchip.com/wwwproducts/devices.aspx?ddocname=en010276

Nordic Semiconductor. (July 2007). nRF24L01 Single Chip 2.4 GHz Transceiver Product Specification, In: *Home, Products, 2.4 GHz RF,* 16.8.2009, Available from: http://www.nordicsemi.com/eng/Products/2.4GHz-RF/nRF24L01

Pallàs-Areny, R. & Webster, J. G. (1999). *Analog Signal Processing*, Wiley, ISBN 0471125288, New York, USA

Spach, M. S., Barr, R. C., Havstad, J. W. & Long, E. C. (1966). Skin-electrode impedance and its effect on recording cardiac potentials. *Circulation*, Vol. 34, No. 4, (October 1966), pp. 649–656, ISSN 1524-4539

Spinelli, E. M., Martinez, N. H., & Mayosky, M. A. (2001). A single-supply biopotential amplifier. *Med. Eng. Phys.*, Vol. 23, No. 3, (April 2001), pp. 235-238, ISSN 1350-4533

Spinelli, E.M., Pallás-Areny, R. & Mayosky, M.A. (2003). AC-coupled front-end for biopotential measurements. *IEEE Transactions on Biomedical Engineering*, Vol. 50, No. 3, (March 2003), pp. 391-395, ISSN: 0018-9294

Task Force of the European Society of Cardiology and the North American Society of Pacing and Electrophysiology. (1996). Heart rate variability: standards of measurement, physiological interpretation and clinical use. *European Heart Journal*, Vol. 17, No. 3, (March 1996), pp. 354-381, ISSN 0195-668X

Thakor, N.V. (1988). Electrocardiographic monitors, In: *Encyclopedia of Medical Devices and Instrumentation*, J.G. Webster, pp. 1002-1017, Wiley, ISBN 0471629693, USA

Weng, B., Blanco-Velasco, M., Barner, K.E. (2006). Baseline wander correction in ECG by the empirical mode decomposition. Bioengineering Conference, 2006, Proceedings of the IEEE 32nd Annual Northeast, 2006, pp. 135-136, ISBN 0-7803-9563-8, May 2006

Winter, B.B. & Webster J.G. (1983). Driven-right leg circuit design. *IEEE Transactions on Biomedical Engineering*, Vol. 30, No.1, (January 1983), pp. 62-66, ISSN: 0018-9294

World Health Organization (WHO). (January 2011). Cardiovascular diseases (CVDs), In: *Media centre, Fact sheet No. 317*, 04.03.2011, Available from:
http://www.who.int/mediacentre/factsheets/fs317/en/index.html
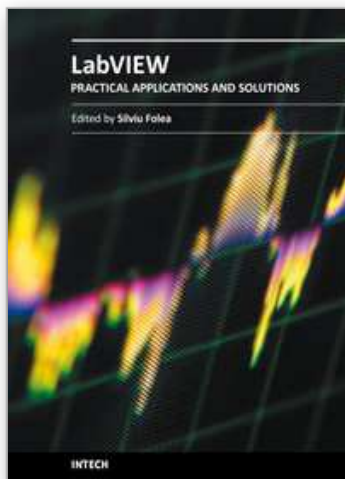
Practical Applications and Solutions Using LabVIEW™ Software

Edited by Dr. Silviu Folea

The book consists of 21 chapters which present interesting applications implemented using the LabVIEW environment, belonging to several distinct fields such as engineering, fault diagnosis, medicine, remote access laboratory, internet communications, chemistry, physics, etc. The virtual instruments designed and implemented in LabVIEW provide the advantages of being more intuitive, of reducing the implementation time and of being portable. The audience for this book includes PhD students, researchers, engineers and professionals who are interested in finding out new tools developed using LabVIEW. Some chapters present interesting ideas and very detailed solutions which offer the immediate possibility of making fast innovations and of generating better products for the market. The effort made by all the scientists who contributed to editing this book was significant and as a result new and viable applications were presented.

How to reference

In order to correctly reference this scholarly work, feel free to copy and paste the following:

Agustín Márquez-Espinoza, José G. Mercado-Rojas, Gabriel Vega-Martínez and Carlos Alvarado-Serrano (2011). ECG Ambulatory System for Long Term Monitoring of Heart Rate Dynamics, Practical Applications and Solutions Using LabVIEW™ Software, Dr. Silviu Folea (Ed.), ISBN: 978-953-307-650-8, InTech, Available from: http://www.intechopen.com/books/practical-applications-and-solutions-using-labview-software/ecg-ambulatory-system-for-long-term-monitoring-of-heart-rate-dynamics

INTECH
open science | open minds